

#  
**27**

*Intensity Noise Performance  
of Semiconductor Lasers*

---

---

---

---

---

---

# **APPLICATION NOTE**

---

Test report: Intensity noise performance of  
semiconductor lasers operated by the  
LDX-3232 current source

Dr. Tobias Gensty  
Prof. Dr. Wolfgang Elsässer

Institute of Applied Physics  
Darmstadt University of Technology

# 1 Introduction

The aim of the test procedure was to study the current noise performance of the novel ILX Lightwave current source LDX-3232. It is a high compliance voltage ( $> 15$  V) current source with a maximum output current of 4000 mA. Therefore, LDX-3232 is capable of driving quantum cascade lasers (QCL) [1]. Typical injection currents and bias voltages to operate QCL in continuous wave operation are in the range of 100–1500 mA and 6–15 V, respectively.

In order to analyze the noise characteristics of LDX-3232, we performed three different measurements. First, we measured the intensity noise of the emitted optical power of a QCL biasing the laser by the LDX-3232 and a self-made low-noise battery current source. Second, we repeated the measurements with a standard telecommunication laser device using four different current sources: LDX-3232, the battery, LDX-3620, and LDC-3744B. Third, we analyzed the current noise of the four current sources directly by detecting the voltage fluctuations across a  $10\ \Omega$  resistor.

In general the results show that the battery current sources (LDX-3620 and self-made battery) yield the best noise performances, i.e. they delivered the lowest current noise and the lasers emitted the lowest intensity noise during the test. The output currents of LDX-3232 and LDC-3744B are noisier compared to the battery current sources resulting in a slightly higher intensity noise of the lasers. Nevertheless, the intensity noise levels of the emitted light were on very low levels with all four current sources showing that these current sources are suitable for applications where a low noise level is required.

This report is organized as follows. In section 2, we describe the experimental setups used for the noise investigations. In section 3, we present the results and discuss the noise properties of the different current sources. And finally in section 4, we conclude the report with a summary of the results and a discussion about the usability of LDX-3232 for laboratory applications.

## 2 Experimental setup

A scheme of the experimental setup for the noise characterization is depicted in Fig. 1. The influence of the current noise on the intensity noise of a laser device is analyzed with the setup shown in Fig. 1(a). For the investigations of the intensity noise properties, we used a distributed feedback (DFB) QCL emitting at a wavelength of  $5.45\ \mu\text{m}$  and a standard telecommunication DFB laser emitting at a wavelength of  $1.55\ \mu\text{m}$ . The lasers were operated in continuous wave operation using different current sources. In the case of the QCL we used:

- ILX LDX-3232 with the 0–2000 mA range
- 24 V battery with  $>30\ \Omega$  internal resistance.

In the case of the standard telecommunication device we used the same two current sources, and additionally:

- ILX LDX-3620 with the 0–200 mA range
- ILX LDC-3744B with the 0–2000 mA range.

The emitted light of both lasers is collected by aspheric lenses and focused onto photovoltaic detectors (D). The bandwidths of the mid-infrared detector for the QCL and the near-infrared detector for the telecommunication device amount to  $\sim 350\ \text{MHz}$  and  $\sim 75\ \text{MHz}$ , respectively. Special care has been taken in order to avoid optical feedback in the experimental setup. The detected photocurrents are separated into the alternating current (AC) and the direct current (DC) by a so-called “Bias-Tee.” The AC part of the signal accounts for the fluctuations of the laser intensity. It is analyzed by an electrical spectrum analyzer after amplification by a low noise amplifier (A). The DC part of the signal gives the photocurrent  $I_{ph}$  which is proportional to the mean optical intensity. The intensity fluctuations are characterized by the relative intensity noise (RIN) which is defined as the ratio of the mean value of the optical intensity fluctuation  $\delta P$  squared to the mean optical power  $P_0$  squared at a specified frequency  $\omega$  in a 1 Hz bandwidth. This ratio can be

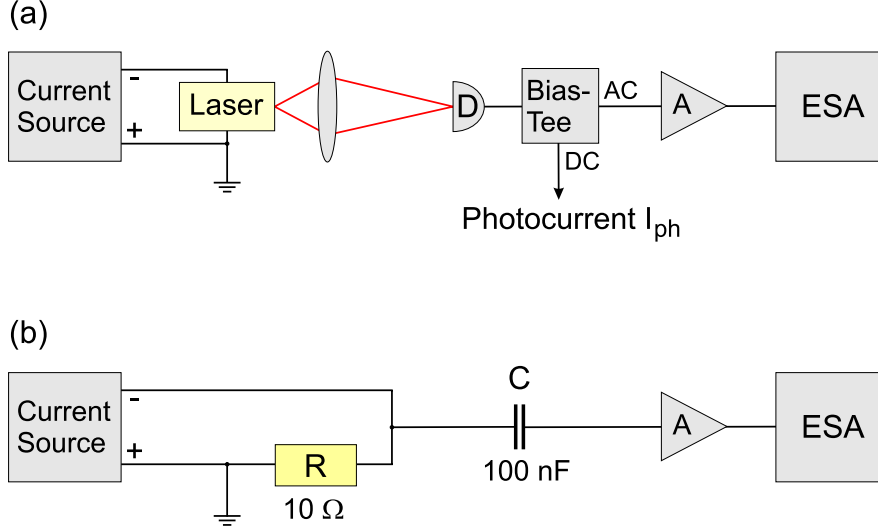


Figure 1: Scheme of the experimental setup for the characterization of (a) the intensity noise of the emitted optical power of a laser device and (b) of the current noise.

expressed as the ratio of the detected electrical powers, thus

$$RIN(\omega) = \frac{S_P(\omega)}{BG I_{ph}^2 R}, \quad (1)$$

where the spectral noise power  $S_P(\omega)$  is the difference between the measured spectral noise power of the signal of the illuminated detector and the spectral dark noise power at the frequency  $\omega$ . The mean electrical power of the detected signal is given by  $I_{ph}^2 R$ . Here,  $R$  is the impedance of the amplifier and  $I_{ph}$  is the photocurrent of the detected signal given by the difference between the photocurrent of the illuminated detector and the dark current, respectively. The resolution bandwidth  $B$  of the ESA gives the normalization to the 1 Hz bandwidth and  $G$  accounts for the gain of the amplifier.

To measure the current noise directly, we used the setup of Fig. 1(b). The current source drives a current through a resistor of  $10\ \Omega$ . The current noise is measured by coupling the voltage fluctuations across the resistor by a  $100\ \text{nF}$  capacitor to a low noise amplifier with an input impedance of  $50\ \Omega$ . The amplified signal is then analyzed by the ESA. In this case we compared the noise power as detected by the ESA of the four current sources: LDX-3232, 24 V battery, LDX-3620, and LDC-3744B.

### 3 Results and Discussion

In the following we will analyze the intensity noise properties in terms of RIN, first, of the QCL, and second, of the standard telecommunication device with respect to the different current sources biasing the laser devices. Then, we will directly compare the current noise of the four current sources as a function of the current.

The RIN measured at a frequency of 50 MHz of the QCL is depicted Fig. 2. The experiment was carried out using the LDX-3232 and the self-made 24 V battery as a current source. In Fig. 2(a) the RIN is plotted as a function of the injection current. The threshold current of the QCL amounts 115 mA and the maximum operation current is 180 mA. To operate this QCL, a bias voltage of around 9 V is needed. With both current sources, RIN decreases with increasing injection current. However, the self-made battery current source yields a lower RIN of the QCL at the same injection current than the LDX-3232. In order to analyze the results in more detail, we compare the RIN as a function of the emitted optical power as depicted in Fig. 2(b). In the case of LDX-3232 as a current source, the measured RIN decreases from -118.7 dB/Hz at an output power of  $P_0 = 0.6$  mW to -148.5 dB/Hz at  $P_0 = 9.2$  mW. This result shows that the QCL yields a good intensity noise performance, i.e. the RIN is on a low level reaching values below -140 dB/Hz, when operated by the LDX-3232. In the case of the battery biasing the QCL, the RIN decreases from -135.4 dB/Hz at  $P_0 = 0.9$  mW to -154.9 dB/Hz at  $P_0 = 8.8$  mW. The RIN of the QCL could be fitted according to a power law as  $RIN \propto P_0^{-\gamma}$ . A least square fit to the experimental data yields  $\gamma = 2.04$ , which is the theoretically expected scaling behavior of RIN of a single-mode QCL with 25 cascaded gain stages [3]. By comparing the observed RIN of the QCL using the two different current sources, we find that the RIN is  $\sim 10$  dB/Hz lower when using the self-made battery instead of LDX-3232. This indicates that the current noise of LDX-3232 is higher than the current noise of the battery resulting in excess noise in the output power of the QCL. From this result we conclude that the self-made battery current source delivers a very quiet injection current whereas LDX-3232 gives some excess noise at a frequency of 50 MHz. Nevertheless, the observed low

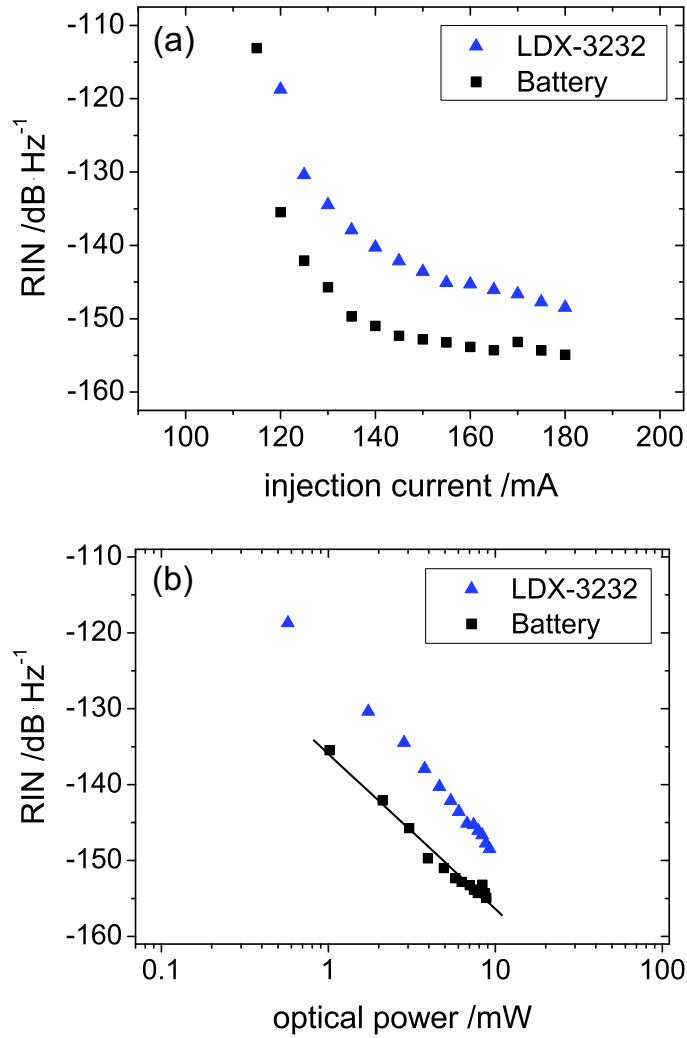


Figure 2: RIN at a frequency of 50 MHz of the QCL biased by the LDX-3232 and the self-made battery as a function of (a) the injection current and (b) the emitted optical power.

intensity noise level of the QCL when using LDX-3232 as a current source shows that LDX-3232 could be used even for applications where a low noise level is required. However, to study the noise properties of the laser itself, a low noise battery current source has to be used.

In order to confirm the results with a conventional interband semiconductor laser, and furthermore, to compare the noise characteristics of a laser operated not only by LDX-3232 and the battery, but also with LDX-3620 and

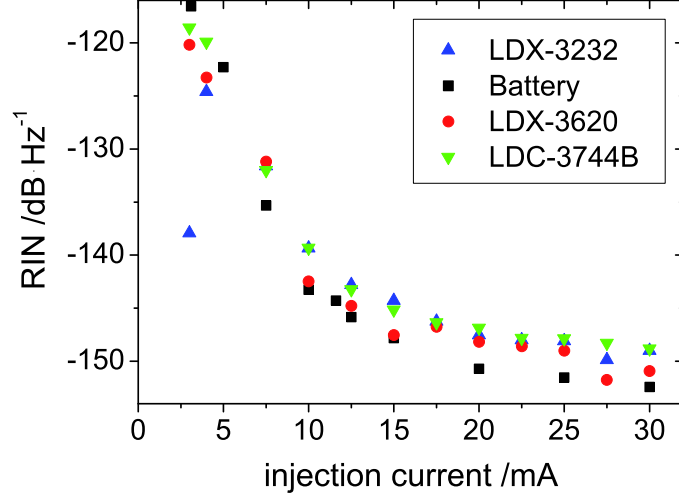


Figure 3: RIN at a frequency of 30 MHz of the standard telecommunication semiconductor laser as a function of the injection current.

LDC-3744B, we have repeated the measurements from above with a standard telecommunication laser device emitting at a wavelength of  $1.55 \mu\text{m}$ . The threshold current of this device amounts to 6 mA. A bias voltage of 1.5–2.5 V is needed to operate this laser. The measured RIN at a frequency of 30 MHz as a function of the injection current is depicted in Fig. 3. For all four current sources, the RIN of the laser decreases with increasing injection current. Above threshold, the lowest RIN is obtained when the laser is operated by the self-made battery. However, we find a comparable intensity noise performance with the LDX-3620. This is not surprising because LDX-3620 is also a battery current source. When using the current sources LDX-3232 and LDC-3744B, the RIN level of the laser is approximately on the same level, but  $\sim 3 \text{ dB/Hz}$  higher than with the battery current sources. These results clearly show that the battery current sources (self-made battery and LDX-3620) yield the lowest RIN levels. Hence, the higher RIN levels of the laser operated by LDX-3232 and LDC-3744B apparently result from a higher current noise level.

In order to compare the current noise of the different current sources directly, we have used the setup depicted in Fig. 1(b). With this setup we measure the current noise induced voltage fluctuations across the resistor. In

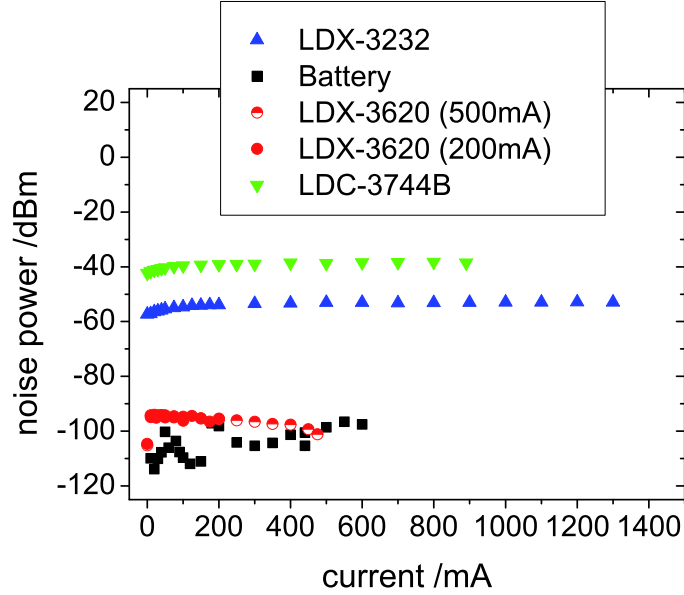


Figure 4: Spectral noise power at a frequency of 50 MHz of the current noise induced voltage fluctuations across a  $10\ \Omega$  resistor as a function of the current. The resolution bandwidth of the ESA was set to 100 kHz.

Fig. 4 the results are shown for LDX-3232, the battery, LDX-3620, and LDC-3744B. The maximum drive currents of the ILX Lightwave current sources were limited by the compliance voltage, whereas the current of the battery was limited by the maximum allowed power dissipation at the potentiometers. For this experiment, we used LDX-3232 as well as LDC-3744B in the 0–2000 mA range and LDX-3620, both, in the 0–200 mA and the 0–500 mA range. The noise performance of LDX-3620 is nearly equal in both setup ranges. The results shown in Fig. 4 clearly demonstrate that at a frequency of 50 MHz the noise power of the battery current sources is about 40–60 dBm below the noise power of the conventional current sources. We obtained the lowest current noise from our self-made battery. The noise power increases from -110 dBm at a current of 10 mA to -97.5 dBm at 600 mA. The increase of the current noise of the battery is due to the reduction of the internal resistance of the current source in order to increase the output current. However, the internal resistance was  $>30\ \Omega$  for all drive currents. The current noise of LDX-3620 is only slightly above the self-made battery. It decreases with



the drive current from -94.9 dBm at 10 mA to -101.1 dBm at 475 mA. The detected noise power of LDX-3232 and LDC-3744B is obviously higher. For LDX-3232, we found that the noise power increases from -57.1 dBm at 10 mA to -52.9 dBm at 1300 mA, and for LDC-3744B, it increases from -41.6 dBm at 10 mA to -38.5 dBm at 890 mA.

This result explains the results obtained for the intensity noise of the laser devices. The current noise of the batteries is so low that we were able to measure the intensity noise properties of the laser devices directly. The higher current noise of the two grid-bound current sources lead to a higher intensity noise of the laser devices. Hence, the QCL as well as the standard telecommunication device showed some excess noise when operated with LDX-3232 or LDC-3744B. However, the higher current noise of LDC-3744B compared to LDX-3232 could not be detected in the intensity noise of the laser.

## 4 Conclusion

We have obtained three major results during the testing procedure. First, we found that the battery-operated current sources delivered the quietest output currents. We have found that the self-made battery current source and LDX-3620 gave a comparable noise performance. The output current noise of LDX-3232 was higher than that of the battery current sources, but still below the one of LDC-3744B. Second, we have observed some excess noise in the output power of the laser devices when operated with LDX-3232 and LDC-3744B. Nevertheless, for injection currents  $\sim 20\%$  above laser threshold, the intensity noise of the laser devices was below -140 dB/Hz, which is a very low noise level. Hence, LDX-3232 is suitable as a current source for QCL in applications where a low noise operation is required. Therefore, LDX-3232 can be regarded as a low noise current source. And third, the usability of LDX-3232 is excellent. The output current is easily adjusted with a precision of 0.1 mA. It offers constant current as well as constant output power operating modes and provides the possibility of current modulation up to a frequency of 250 kHz. Furthermore, LDX-3232 offers various laser protection mechanisms such as a selectable current and compliance voltage

limits and intermittent contact protection. These laser protection features are in particular important for expensive laser devices as QCL. Thus, LDX-3232 is very well suited for laboratory applications of QCL and other laser devices.

## References

- [1] J. Faist, F. Capasso, D. L. Sivco, C. Sirtori, A. L. Hutchinson, and A. Y. Cho, “Quantum cascade laser,” *Science* **264**, 553–556 (1994).
- [2] T. Gensty, W. Elsässer, and Ch. Mann, “Intensity noise properties of quantum cascade lasers,” *Opt. Express* **13**, 2032–2039 (2005), <http://www.opticsexpress.org/abstract.cfm?URI=OPEX-13-6-2032>.
- [3] T. Gensty and W. Elsässer, “Semiclassical model for the relative intensity noise of intersubband quantum cascade lasers,” *Opt. Commun.* **256**, 171–183 (2005).

## White Papers

- A Standard for Measuring Transient Suppression of Laser Diode Drivers
- Degree of Polarization vs. Poincaré Sphere Coverage
- Improving Splice Loss Measurement Repeatability
- Laser Diode Burn-In and Reliability Testing
- Power Supplies: Performance Factors Characterize High Power Laser Diode Drivers
- Reliability Counts for Laser Diodes
- Reducing the Cost of Test in Laser Diode Manufacturing

## Technical Notes

- Attenuation Accuracy in the 7900 Fiber Optic Test System
- Automatic Wavelength Compensation of Photodiode Power
- Measurements Using the OMM-6810B Optical Multimeter
- Bandwidth of OMM-6810B Optical Multimeter Analog Output
- Broadband Noise Measurements for Laser Diode Current Sources
- Clamping Limit of a LDX-3525 Precision Current Source
- Control Capability of the LDC-3916371 Fine Temperature Resolution Module
- Current Draw of the LDC-3926 16-Channel High Power Laser Diode Controller
- Determining the Polarization Dependent Response of the FPM-8210 Power Meter
- Four-Wire TEC Voltage Measurement with the LDT-5900 Series Temperature Controllers
- Guide to Selecting a Bias-T Laser Diode Mount
- High Power Linearity of the OMM-6810B and OMH-6780/6790/6795B Detector Heads
- Large-Signal Frequency Response of the 3916338 Current Source Module
- Laser Wavelength Measuring Using a Colored Glass Filter
- Long-Term Output Drift of a LDX-3620 Ultra Low-Noise Laser Diode Current Source
- Long-Term Output Stability of a LDX-3525 Precision Current Source
- Long-Term Stability of an MPS-8033/55 ASE Source
- LRS-9424 Heat Sink Temperature Stability When Chamber Door Opens
- Measurement of 4-Wire Voltage Sense on an LDC-3916 Laser Diode Controller
- Measuring the Power and Wavelength of Pulsed Sources Using the OMM-6810B Optical Multimeter
- Measuring the Sensitivity of the OMH-6709B Optical Measurement Head
- Measuring the Wavelength of Noisy Sources Using the OMM-6810B Optical Multimeter
- Output Current Accuracy of a LDX-3525 Precision Current Source
- Pin Assignment for CC-305 and CC-505 Cables
- Power and Wavelength Stability of the 79800 DFB Source Module
- Power and Wavelength Stability of the MPS-8000 Series Fiber Optic Sources
- Repeatability of Wavelength and Power Measurements Using the OMM-6810B Optical Multimeter
- Stability of the OMM-6810B Optical Multimeter and OMH-6727B InGaAs Power/Wavehead
- Switching Transient of the 79800D Optical Source Shutter
- Temperature Controlled Mini-DIL Mount
- Temperature Stability Using the LDT-5948
- Thermal Performance of an LDM-4616 Laser Diode Mount
- Triboelectric Effects in High Precision Temperature Measurements
- Tuning the LDP-3840 for Optimum Pulse Response
- Typical Long-Term Temperature Stability of a LDT-5412 Low-Cost TEC
- Typical Long-Term Temperature Stability of a LDT-5525 TEC
- Typical Output Drift of a LDX-3412 Low-Cost Precision Current Source
- Typical Output Noise of a LDX-3412 Precision Current Source

- Typical Output Stability of the LDC-3724B
- Typical Output Stability of a LDX-3100 Board-Level Current Source
- Typical Pulse Overshoot of the LDP-3840/03 Precision Pulse Current Source
- Typical Temperature Stability of a LDT-5412 Low-Cost Temperature Controller
- Using Three-Wire RTDs with the LDT-5900 Series Temperature Controllers
- Voltage Drop Across High Current Laser Interconnect Cable
- Voltage Drop Across High Current TEC Interconnect Cable
- Voltage Limit Protection of an LDC-3916 Laser Diode Controller
- Wavelength Accuracy of the 79800 DFB Source Module

## Application Notes

- App Note 1: Controlling Temperatures of Diode Lasers and Detectors Thermoelectrically
  - App Note 2: Selecting and Using Thermistors for Temperature Control
  - App Note 3: Protecting Your Laser Diode
  - App Note 4: Thermistor Calibration and the Steinhart-Hart Equation
  - App Note 5: An Overview of Laser Diode Characteristics
  - App Note 6: Choosing the Right Laser Diode Mount for Your Application
  - App Note 8: Mode Hopping in Semiconductor Lasers
  - App Note 10: Optimize Testing for Threshold Calculation Repeatability
  - App Note 11: Pulsing a Laser Diode
  - App Note 12: The Differences between Threshold Current Calculation Methods
  - App Note 13: Testing Bond Quality by Measuring Thermal Resistance of Laser Diodes
  - App Note 14: Optimizing TEC Drive Current
  - App Note 17: AD590 and LM335 Sensor Calibration
  - App Note 18: Basic Test Methods for Passive Fiber Optic Components
  - App Note 20: PID Control Loops in Thermoelectric Temperature Controllers
  - App Note 21: High Performance Temperature Control in Laser Diode Test Applications
  - App Note 22: Modulating Laser Diodes
  - App Note 23: Laser Diode Reliability and Burn-In Testing
  - App Note 25: Novel Power Meter Design Minimizes Fiber Power Measurement Inaccuracies
-

---

For application assistance or additional information on our products or services you can contact us at:

**ILX Lightwave Corporation**

31950 Frontage Road, Bozeman, MT 59715

Phone: 406-556-2481 • 800-459-9459 • Fax: 406-586-9405

Email: [sales@ilxlightwave.com](mailto:sales@ilxlightwave.com)

To obtain contact information for our international distributors and product repair centers or for fast access to product information, technical support, LabVIEW® drivers, and our comprehensive library of technical and application information, visit our website at:

**[www.ilxlightwave.com](http://www.ilxlightwave.com)**

